Journal of Analytical Science and Technology

SHORT REPORT

Open Access

Laser ablation MC-ICPMS U-Th and U-Th-Pb dating of Quaternary zircons from Jeju Island, Korea

Youn-Joong Jeong[1], Min-Ji Jung[1,2], Ung-San Ahn[3] and Albert Chang-sik Cheong[1,2*]

Abstract

Background Laser ablation inductively coupled plasma mass spectrometry (LA-ICPMS) emerged in the mid-1980s and rapidly became a crucial dating tool. The advent of femtosecond LA systems has substantially reduced volatility-dependent mass fractionation. This study showcases U-Th and U-Th-Pb dating results of Quaternary zircons collected from Jeju Island, Korea, utilizing an advanced femtosecond laser-connected multi-collector (MC)-ICPMS.

Findings Zircon grains from trachyte samples near the Baeknokdam lake (JJ616-1), Yeongsil (JJ08-1), Chunwangsa (JJ09-1), and Oraidong (JJ09-3) provided weighted mean ^{238}U-^{230}Th ages of 28.7 ± 1.6 ka (n = 56/64, MSWD = 3.8), 81.8 ± 10.9 ka (n = 11/12, MSWD = 1.6), 92.6 ± 4.6 ka (n = 49/51, MSWD = 2.2), and 117.6 ± 8.2 ka (n = 48/50, MSWD = 3.2), respectively. The age determination for JJ08-1 zircon aligned well with the recommended value (82 ± 6 ka). Zircons from Sanbangsan (JJ615-1) and Wonmansa (JJ08-2) trachytes yielded common Pb and radioactive disequilibrium-corrected weighted mean ^{238}U-^{206}Pb ages of 785 ± 5 ka (n = 27/28, MSWD = 0.90) and 743 ± 8 ka (n = 28/30, MSWD = 0.79), respectively. The weighted mean ^{238}U-^{206}Pb ages of Penglai and 61.308 reference zircons were determined to be 4226 ± 21 ka (n = 22/25, MSWD = 3.8) and 2488 ± 20 ka (n = 19/20, MSWD = 1.8), respectively. These ages are concordant with the recommended values.

Conclusions Our data provides additional evidence of trachyte magmatism occurring in Jeju Island during the transitional period between the Early and Middle Pleistocene and the Late Pleistocene. The zircon samples analyzed in this study could serve as reference age data for Quaternary geochronology research.

Keywords Zircon, Jeju Island, LA-ICPMS, U-Th age, U-Th-Pb age

Introduction

In the 1980s, the concept of coupling a laser ablation (LA) system with an inductively coupled plasma mass spectrometer (ICPMS) was introduced (Gray 1985). In LA-ICPMS analysis, a pulsed laser is used to ablate the surface of the sample within a gas-tight chamber, creating a stream of aerosol carried to an ICP source. Within the ICP source, the aerosol is vaporized and converted into ions. These ions are then separated according to their mass-to-charge ratios using a mass analyzer and quantified by a detector. Throughout these processes, elemental and isotopic fractionation is inevitable due to various factors, such as differences in elemental volatility and transportability, and time-dependent changes in particle size distribution (Hirata and Nesbitt 1995; Guillong and Günther 2002; Hirata 2003; Jackson and Günther 2003; Jackson et al. 2004).

Over the past few decades, significant instrumental and strategic advancements have addressed these challenges

*Correspondence:
Albert Chang-sik Cheong
ccs@kbsi.re.kr
[1] Korea Basic Science Institute, Cheongju 28119, Republic of Korea
[2] Graduate School of Analytical Science and Technology, Chungnam National University, Daejeon 34134, Republic of Korea
[3] World Heritage Office, Jeju Special Self-Governing Province, Jeju, Republic of Korea

and enhanced the capabilities of LA-ICPMS (Sylvester and Jackson 2016). The use of helium has improved the transport of ablated aerosols to the ICP, leading to increased signal intensities. The introduction of a two-volume sample chamber design has provided rapid signal response, effectively reducing positional bias and enabling higher spatial resolution. Additionally, the reduction in laser wavelength has resulted in higher absorption and improved ablation of transparent materials, as well as more efficient ionization in the ICP. The initial generation of laser ablation system utilized long wavelength, visible laser beams (Gray 1985), but it was soon recognized that the shorter wavelength, particularly the 213 nm Nd:YAG and 193 nm ArF Excimer, offered more efficient and stable ablation of geologic materials. In the 2000s, the introduction of femtosecond lasers proved highly effective in reducing target heating and minimizing volatility-dependent elemental and isotopic fractionation. This advancement resulted in several benefits, such as higher evaporation efficiency and a shift in the size distribution of sample particles toward smaller sizes, thus enhancing the precision and accuracy of data (Russo et al. 2002; Poitrasson et al. 2003; Diwakar et al. 2013). The application of femtosecond laser technology would be particularly beneficial for absolute element concentration determinations and stable metal and metalloid isotope analyses (Poitrasson and d'Abzac 2017).

The pioneering work of Feng et al. (1993) and Fryer et al. (1993), based on $^{207}Pb/^{206}Pb$ determinations on Precambrian zircon, showcased the utility of LA-ICPMS as a dating tool. The versatility, ease-of-use, speed, and relatively moderate cost of LA-ICPMS addressed a significant challenge in ion probe dating—the high expense of instrumentation and the limited availability of suitably equipped laboratories. Since the mid-1990s, continuous advancements in the laser system and ICPMS instrumentation have facilitated the dating of zircon and other accessory minerals using the Pb/U decay scheme (Woodhead et al. 2016). The challenges associated with LA-ICPMS U-Pb geochronology, particularly the fractionation of Pb relative to U during ablation, transport, and ionization processes, as well as common Pb correction difficulties, have been extensively discussed (e.g., Jackson et al. 2004). The present-day spatial resolution, and potentially precision, in ^{238}U-^{206}Pb age determination have become nearly comparable to that achieved by the ion probe technique, provided that well-characterized matrix-matched reference materials are available (Woodhead et al. 2016).

The dating of Quaternary zircon through in situ U-Th analysis began in the 1990s, employing the ion probe technique (e.g., Reid et al. 1997). While the potential of LA-ICPMS in U-Th analysis of zircon was recognized early on (Stirling et al. 2000), its widespread adoption came much later (Bernal et al. 2014). In situ U-Pb dating of Quaternary zircon commenced earnestly in the 2000s using the ion probe (Bacon et al. 2000). Given the analytical challenges in U-Th and U-Pb dating for Quaternary zircon, stemming from extremely small amounts of radiogenic daughter nuclides in the decay chains, the instrumental bias should be corrected with a great care. The use of appropriate mineral standards is critical not only for correcting mass bias and elemental fractionation, but also for ensuring the overall accuracy and reliability of LA-ICPMS age determinations. As part of our effort to develop reference materials, we present the results of U-Th and U-Th-Pb dating for Pleistocene zircons collected from Jeju volcanic island, Korea, using an advanced femtosecond laser-connected multi-collector (MC)-ICPMS.

Principles of zircon U-Th and U-Th-Pb dating

The principles of zircon U-Th and U-Th-Pb dating are well-explained in textbooks (e.g., Faure and Mensing 2005), and only briefly reminded here.

The radioactivity of ^{230}Th in zircon is attributed to two components. Firstly, there is the excess ^{230}Th decay, expressed as $(^{230}\mathrm{Th})^0_{\mathrm{excess}}\ e^{-\lambda t}$ (λ is the decay constant of $^{230}\mathrm{Th} = 9.1706 \times 10^{-6}\ \mathrm{y}^{-1}$), with a half-life of 75,584 ± 110 years (Cheng et al. 2013). Secondly, there is the activity of supported ^{230}Th, represented as $(^{238}\mathrm{U})(1 - e^{-\lambda t})$, which increases with time. On the $^{230}Th/^{232}Th$ (activity ratio, y-axis) and $^{238}U/^{232}Th$ (activity ratio, x-axis) plot, zircon data conform to a linear relationship (isochron) with a slope of $1 - e^{-\lambda t}$ and a y-intercept of $(^{230}\mathrm{Th}/^{232}\mathrm{Th})^0_{\mathrm{excess}}\ e^{-\lambda t}$ provided that the analyzed parts of the zircon share the same age and initial $^{230}Th/^{232}Th$ ratio, and have remained closed to U and Th after crystallization. After approximately 5 times the ^{230}Th half-life (over 350,000 years), a state of secular equilibrium is re-established, resulting in all data points aligning along the 1:1 line (equiline) of the $^{230}Th/^{232}Th$-$^{238}U/^{232}Th$ diagram. Consequently, the information needed for zircon U-Th disequilibrium dating is the $^{230}Th/^{232}Th$ and $^{238}U/^{232}Th$ ratios.

In the case of old zircon that has attained secular equilibrium among radionuclides in the U-Th-Pb decay chains, the production rates of Pb isotopes at the end of the chains become equal to the decay rates of their respective grandparent nuclides. Consequently, the decay of U and Th isotopes can be treated as if they directly transform into Pb isotopes. However, for young (i.e., Pliocene or younger) zircon, one must consider isotope fractionation effects involving intermediate daughters such as ^{230}Th and ^{231}Pa. Zircon has the tendency to exclude a significant proportion of ^{230}Th in the magma. As a result, after decay, there will be a deficiency in ^{206}Pb, leading to the underestimation of the ^{238}U-^{206}Pb age. This effect was already recognized as early as the 1970s (Mattinson 1973; Ludwig 1977) and quantified by Schärer (1984) with Eq. (1).

$$^{206}\mathrm{Pb} = {}^{238}\mathrm{U}\left[(e^{\lambda_{238}t} - 1) + (\lambda_{238}/\lambda_{230})(f_{\mathrm{Th/U}} - 1)\right] \quad (1)$$

where $f_{Th/U} = [Th/U]_{concentration,\ zircon}/[Th/U]_{concentration,\ magma}$, λ_{238} = decay constants of $^{238}U = 1.55125 \times 10^{-10}\ y^{-1}$ (Steiger and Jäger 1977), λ_{230} = decay constants of $^{230}Th = 9.1706 \times 10^{-6}\ y^{-1}$ (Cheng et al. 2013) and t = age.

More recently, Sakata (2018) proposed a practical approach for calculating the corrected U-Pb age of Quaternary zircon. This scheme is a kind of ^{207}Pb-correction method based on a modified Tera-Wasserburg concordia. Since zircon typically crystallizes in intermediate to felsic magma, the influence of melt disequilibria can be reasonably neglected. In this case, the modified concordia is constructed using Eqs. (2) and (3) (Sakata et al. 2017). A bisection method between the modified concordia and the common Pb line can be used to calculate the ^{238}U-^{206}Pb age corrected for the contributions from both initial disequilibria and common Pb, and its uncertainty.

$$\left(^{206}\mathrm{Pb}/^{238}\mathrm{U}\right) = (e^{\lambda_{238}t} - 1) + (\lambda_{238}/\lambda_{230})\left(f_{\mathrm{Th/U}} - 1\right)(1 - e^{-\lambda_{230}t})e^{\lambda_{238}t} \quad (2)$$

$$\left(^{207}\mathrm{Pb}/^{235}\mathrm{U}\right) = (e^{\lambda_{235}t} - 1) + (\lambda_{235}/\lambda_{231})\left(f_{\mathrm{Pa/U}} - 1\right)(1 - e^{-\lambda_{231}t})e^{\lambda_{235}t} \quad (3)$$

where $f_{Pa/U} = [Pa/U]_{zircon}/[Pa/U]_{magma}$, λ_{235} = decay constants of $^{235}U = 9.8485 \times 10^{-10}\ y^{-1}$ (Steiger and Jäger 1977), λ_{231} = decay constants of $^{231}Pa = 2.13 \times 10^{-5}\ y^{-1}$ (Lide and Frederikse 1995) and t = age.

For instance, consider a 1 Ma zircon without common Pb and featuring a Th/U ratio five times lower than that of the melt ($f_{Th/U} = 0.2$). The difference between disequilibrium-corrected and uncorrected ^{238}U-^{206}Pb ages for this zircon reaches approximately 9%, significantly surpassing the bounds of analytical uncertainty.

Geology of Jeju Island and sample collection

Jeju Island, the largest island in Korea, is situated on the continental shelf around 80 km off the south coast of the Korean Peninsula (Fig. 1). The volcanic activity on Jeju Island began during the Early Pleistocene, approximately 1.7 million years ago. The island has been shaped

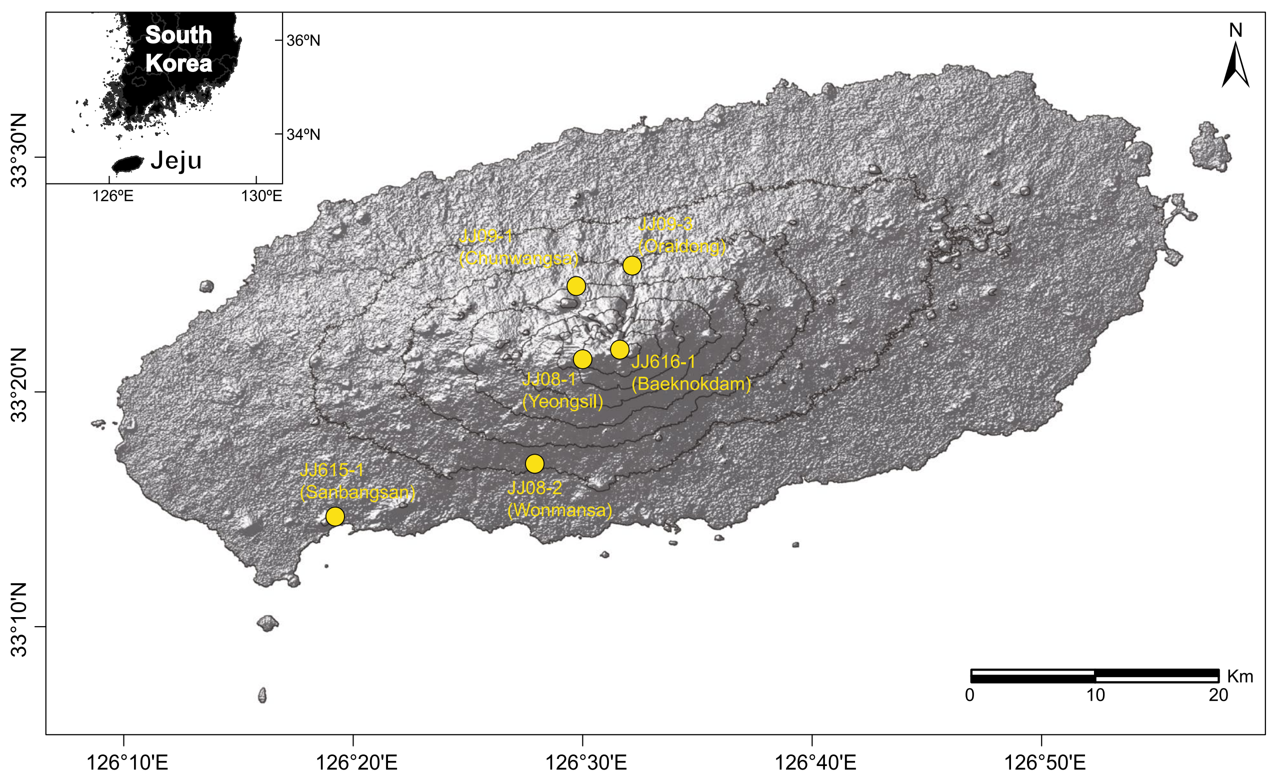

Fig. 1 Digital elevation model of Jeju Island based on ASTER satellite data acquired on 30 November, 2013, with sample locations

by quasi-continuous small-volume volcanism and intermittent large-volume lava effusion. This has resulted in the formation of an elongated symmetrical shield volcano with Mt. Halla at its summit, accompanied by over 300 monogenetic scoria cones, as well as minor tephra rings, maars, and lava domes. Geochronological and geochemical analyses suggest that Jeju volcanic rocks can be divided into three geochemically distinct groups: the Early-Middle Pleistocene high-Al alkalic magma suite (Stage 1), the Middle Pleistocene transitional alkalic magma suite (Stage 2), and the Middle to Late Pleistocene low-Al alkalic magma suite (Stage 3) (Brenna et al. 2015, and references therein). Presently, the island's surface is predominantly covered with rocks from Stage 3 volcanism. Studies employing optically stimulated luminescence and radiocarbon dating have confirmed that volcanic activity persisted into the Holocene (Yeo et al. 2019, and references therein).

In this study, six trachyte samples were collected from inner areas and the outer rim of the island, as shown in Fig. 1. The sampling sites include outcrops near Sanbangsan (sample JJ615-1), the Baeknokdam lake at the summit of Mt. Halla (JJ616-1), Yeongsil (JJ08-1), Wonmansa (JJ08-2), Chunwangsa (JJ09-1), and Oraidong (JJ09-3). Drawing from previously published age data (Koh et al., 2013; Marsden et al. 2021), we presume that the Sanbangsan and Wonmansa trachytes formed during Stage 1, whereas the Baeknokdam, Yeongsil, and Chunwangsa trachytes are associated with Stage 3. The age of the Oraidong trachyte remains undetermined. Additional file 1: Table S1 provides detailed information about these trachytes, encompassing the GPS coordinates, rock types, mineralogy, and texture.

Analytical methods

The major and trace element concentrations of the trachyte whole-rocks were analyzed at Actlabs (Canada) using the combination of X-ray fluorescence spectrometry for fused glass beads and quadrupole ICPMS and ICP optical emission spectrometry for dissolved solutions of the beads.

Zircon grains were extracted through conventional sieving, magnetic, and heavy liquid techniques, and then embedded in epoxy along with reference materials including the 91500, 61.308 (Wiedenbeck et al. 1995, 2004), Plešovice (Sláma et al. 2008), Penglai (Li et al. 2010), FC-1 (Paces and Miller Jr 1993), Temora 2 (Black et al. 2004), and LKZ-1 (Cheong et al. 2019) zircons. The polished surfaces of the zircons were analyzed using a scanning electron microscopy (JEOL JSM-6610LV) at the Korea Basic Science Institute (KBSI) to obtain cathodoluminescence (CL) and backscattered electron images. For isotopic analysis of U, Th, and Pb, a Plasma II MC-ICPMS (Nu Instruments) with a 257 nm femtosecond LA system (Excite Pharos, Teledyne Cetac) was utilized at the KBSI. The instrument's operational parameters are summarized in Additional file 2: Table S2. The obtained data were processed using the Iolite 2.5 software within the Igor Pro 6.3.5.5 program (Paton et al. 2011). Weighted mean ages were calculated using the Isoplot 3.75 program (Ludwig 2012) and are reported at the 95% confidence level.

For zircon U-Th dating, signal intensities were simultaneously measured using Faraday collectors (for ^{238}U and ^{232}Th) and ion counters (for ^{230}Th and 228 mass). The measured $^{238}U/^{232}Th$ ratios were corrected based on the recommended values of the 91500 zircon ([U] = 80.0 μg/g, [Th] = 29.9 μg/g; Wiedenbeck et al. 2004). The ^{238}U and ^{232}Th counts of the 91500 zircon were employed to approximately determine U and Th concentrations in the sample spots. The peak intensity of 228 mass was used for correcting the contribution of molecular zirconium sesquioxide ions to the ^{230}Th peak (Guillong et al. 2015, 2016; 230 mass $= {}^{90}Zr^{92}ZrO_3^{+} + {}^{91}Zr_2O_3^{+} = 0.7142 \times 228$ mass $(= {}^{90}Zr_2O_3^{+})$, while maintaining ThO^+/Th^+ below 0.005. The peak tail of ^{232}Th, the relative sensitivity between U and Th, and the Faraday-ion counter efficiency were collectively corrected based on the assumption that the Plešovice zircon ($^{206}Pb/^{238}U$ age = 337 Ma; Sláma et al. 2008) is in ^{238}U-^{230}Th secular equilibrium. Radioactivity ratios were calculated using the decay constants proposed by Steiger and Jäger (1977) (for ^{238}U and ^{232}Th) and Cheng et al. (2013) (for ^{230}Th). After implementing the necessary corrections and calibrations, we confirmed that the radioactivity ratios of ($^{230}Th/^{232}Th$) and ($^{238}U/^{232}Th$) for the 91500, FC-1, Temora 2, and LKZ-1 standards plotted on the equiline (Additional file 6: Fig. S1).

For U-Th-Pb dating, signal intensities were measured simultaneously with Faraday collectors (for ^{238}U and ^{232}Th) and ion counters (for $^{208, 207, 206, 204}Pb$ and ^{202}Hg). To ensure accurate representation of rapidly transient signals during LA sampling, a peak hopping protocol was implemented. Instrumental mass bias and elemental fractionation, as well as Faraday-ion counter efficiency, were collectively calibrated against the 91500 zircon data. The isotopic ratios of the 91500 zircon reported in Wiedenbeck et al. (1995) were used for this calibration. Each analysis cycle comprised 30 s of measuring the instrumental background by analyzing the carrier gas, followed by a 30-s ablation event, resulting in a total analysis time of approximately 2 min.

Results and discussion

Whole-rock composition

Additional file 3: Table S3 presents the chemical compositions of the trachyte whole-rocks. The SiO_2 contents in these samples range from 59.38 to 65.16 wt. %, accompanied by corresponding total alkali contents ($Na_2O + K_2O$) ranging from 9.12 to 11.33 weight %. Following the naming scheme of Middlemost (1994), the trachyte samples are designated as either trachyandesite (sample JJ09-3) or trachyte (for the other samples). Based on the K_2O versus SiO_2 relationship (Le Maitre et al. 1989), these samples consistently belong to the shoshonite series. The observed enrichment of large-ion-lithophile elements relative to mid-oceanic ridge basalts and light rare earth element-enriched chondrite-normalized pattern align with the general characteristics of oceanic island basalts (Sun and McDonough 1989). The Th/U ratios span a relatively narrow range between 3.91 and 4.85.

Zircon morphology and CL texture

Figure 2 displays representative CL images of separated zircon grains. The majority of the grains exhibit CL textures that indicate their primary magmatic origin, and they remain mostly non-metamict, unaltered, and lacking xenocrystic cores. Zircon crystals from sample JJ615-1 are transparent or translucent, appearing as euhedral to subhedral prismatic shards with lengths of up to 200 μm. Under CL, they display sector or banded zoning, upon which oscillatory zoning is imposed. While some shards are unzoned and appear homogeneous in CL, most exhibit clear zoning patterns. In contrast, JJ616-1 zircons are transparent and vary in shape from equant to prismatic crystals, ranging in length from approximately 150 to 300 μm. The majority of these grains show evident oscillatory zoning under CL. Zircons from sample JJ08-1 appear transparent or pale brown in color, exhibiting euhedral to subhedral crystal faces with lengths ranging between 100 and 200 μm. Most grains show faint to clear oscillatory zoning, while some display resorption patterns. Needle-shaped inclusions, likely apatite, are frequently observed within the grains. Zircons in sample JJ08-2 are transparent to translucent pale brown crystals, varying in size from < 50 to 300 μm. The grains exhibit euhedral to anhedral faces, and most of them display clear or faint oscillatory zoning under CL. Zircons from sample JJ09-1 are long prismatic euhedral grains, with lengths reaching up to 300 μm. Needle-shaped inclusions are frequently observed within the grains. Under CL, oscillatory or sector zoning is observed in most grains. JJ09-3 zircons are mostly transparent, appearing as euhedral prismatic or subhedral crystals, with lengths between 100 and 200 μm. Sector or oscillatory zoning is observed under CL, and some grains contain needle-shaped inclusions.

U-Th dating

The U-Th concentrations and radioactivity ratios of the zircons are provided in Additional file 4: Table S4. Zircons from sample JJ616-1 near the Baeknokdam lake exhibit moderate to high U (525 ± 252 μg/g, one standard deviation, same hereafter unless otherwise noted) and Th (653 ± 469 μg/g) concentrations, with ($^{238}U/^{232}Th$) activity ratios ranging from 1.74 to 4.06. These zircons yield a weighted mean ^{238}U-^{230}Th age of 28.7 ± 1.6 ka (n = 56/64, mean squared weighted deviation (MSWD) = 3.8) as shown in Fig. 3. Considering the preserved typical igneous texture in these zircons, as well as in those from other samples (Fig. 2), this age is believed to represent the magmatic crystallization. Previous studies near Baeknokdam lake have utilized various dating methods, such as optically stimulated luminescence (Ahn and Hong 2017) and the zircon double dating method (Marsden et al. 2021), which combines U-Th-Pb and (U-Th)/He techniques. The results of these studies ranged from 78 to 2 ka, with a concentrated population between approximately 30 and 20 ka. Our data further support the significance of ~ 30 ka magmatism in the formation of trachyte magma beneath Mt. Halla.

Zircons from sample JJ08-1 yield a weighted mean ^{238}U-^{230}Th age of 81.8 ± 10.9 ka (n = 11/12, MSWD = 1.6) (Fig. 3), with moderate U (428 ± 343 μg/g) and Th (440 ± 367 μg/g) concentrations. Sample JJ08-1 was taken from the same outcrop containing the SS14-28 zircon standard, which has a recommended ^{238}U-^{230}Th age of 82 ± 6 ka (Marsden et al. 2022). Our data provide additional analytical results supporting that age.

JJ09-1 zircons provide a weighted mean ^{238}U-^{230}Th age of 92.6 ± 4.6 ka (n = 49/51, MSWD = 2.2) (Fig. 3), with moderate U (307 ± 197 μg/g) and Th (299 ± 366 μg/g) concentrations. The sampling locality is the same as for sample HS100-5 in Marsden et al. (2021), which yielded comparable U-Th dates ranging from 87 ± 23 to 168 ± 117 ka, with a mean of 111 ± 14 ka. Zircons from sample JJ09-3 yield a slightly older weighted mean ^{238}U-^{230}Th age of 117.6 ± 8.2 ka (n = 48/50, MSWD = 3.2) (Fig. 3). They also have moderate U (263 ± 188 μg/g) and Th (295 ± 284 μg/g) concentrations.

Our U-Th zircon ages further support the Late Pleistocene magmatic events on Jeju Island as revealed by previous studies (Koh et al. 2013; Marsden et al. 2021).

U-Th-Pb dating

The zircon U-Th-Pb isotope data are listed in Additional file 5: Table S5. The results are discussed below, considering common Pb and radioactive disequilibrium correction.

For the Penglai reference zircon, the $f_{Th/U}$ (Eq. 1) varies from 0.07 to 0.15, with an average of 0.12 ± 0.03,

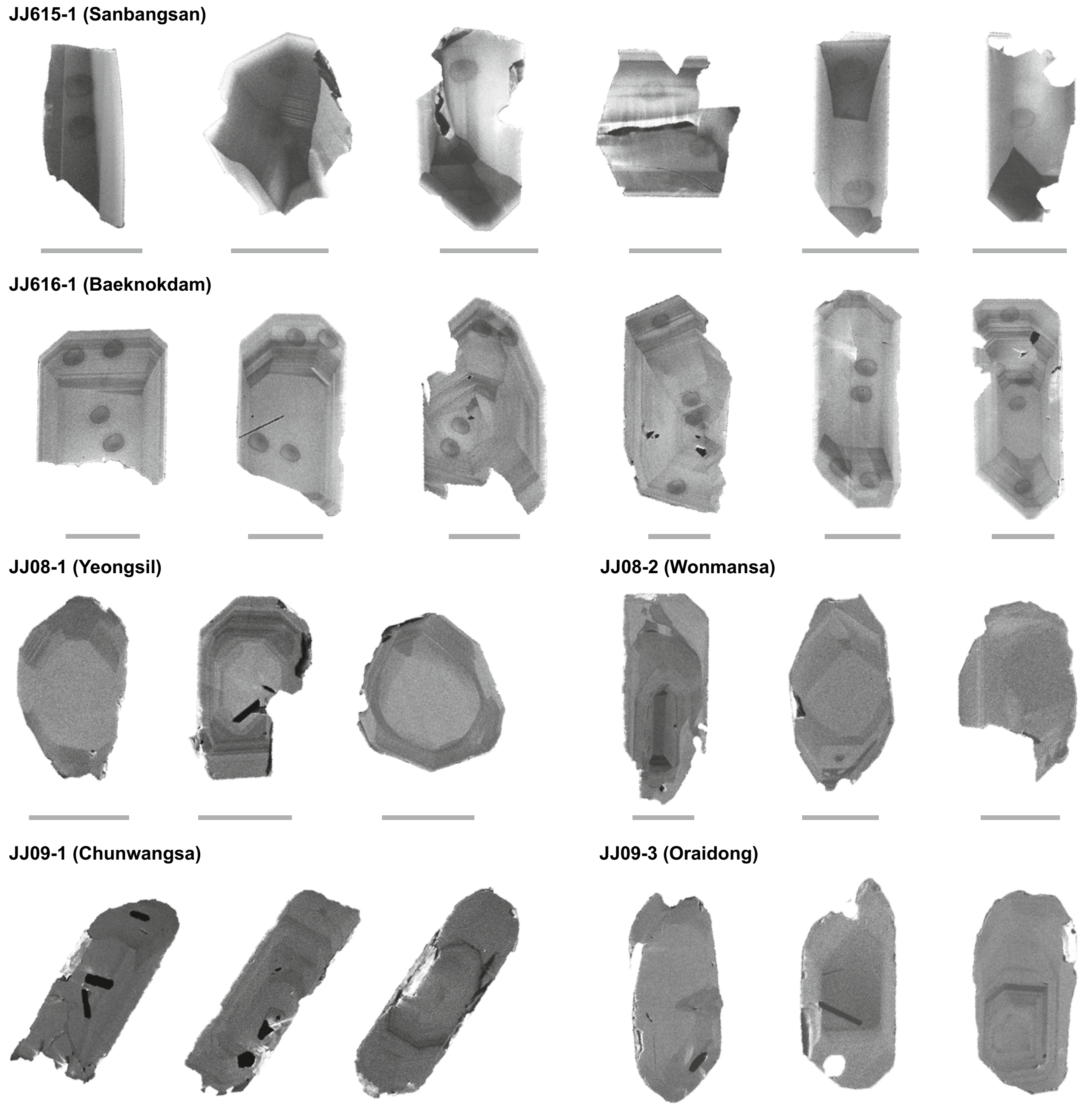

Fig. 2 Representative cathodoluminescence images of Jeju zircons. Scale bars represent 100 µm. Certain grains from samples JJ615-1 and JJ616-1 exhibit remnants of analytical spots

assuming that the magma Th/U ratio is the same as that reported for the host basalt (Th/U = 4.09; Ho et al. 2000). Applying the scheme proposed by Sakata (2018), the disequilibrium- and common Pb-corrected weighted mean ^{238}U-^{206}Pb age is determined to be 4,226 ± 21 ka (n = 22/25, MSWD = 3.8), as shown in Fig. 4. In this calculation, 30% error was assigned to $f_{Th/U}$. The $f_{Pa/U}$ (Eq. 3) and common $^{207}Pb/^{206}Pb$ ratio were assumed to be 3.50 ± 1.05 and 0.84 ± 0.05, respectively. This corrected age aligns well with the recommended ^{238}U-^{206}Pb age of 4.29 ± 0.05 Ma, as recently reported by further evaluation for the Penglai zircon (Yu et al. 2020). The fraction of common ^{206}Pb ($f^{206}Pb_c$), based on the $^{207}Pb/^{206}Pb$ ratio on the normal concordia at the corrected ^{238}U-^{206}Pb age, ranges from 5 to 15%. Notably, considering only the $f^{206}Pb_c$, the ^{238}U-^{206}Pb dates yield a distinctly younger

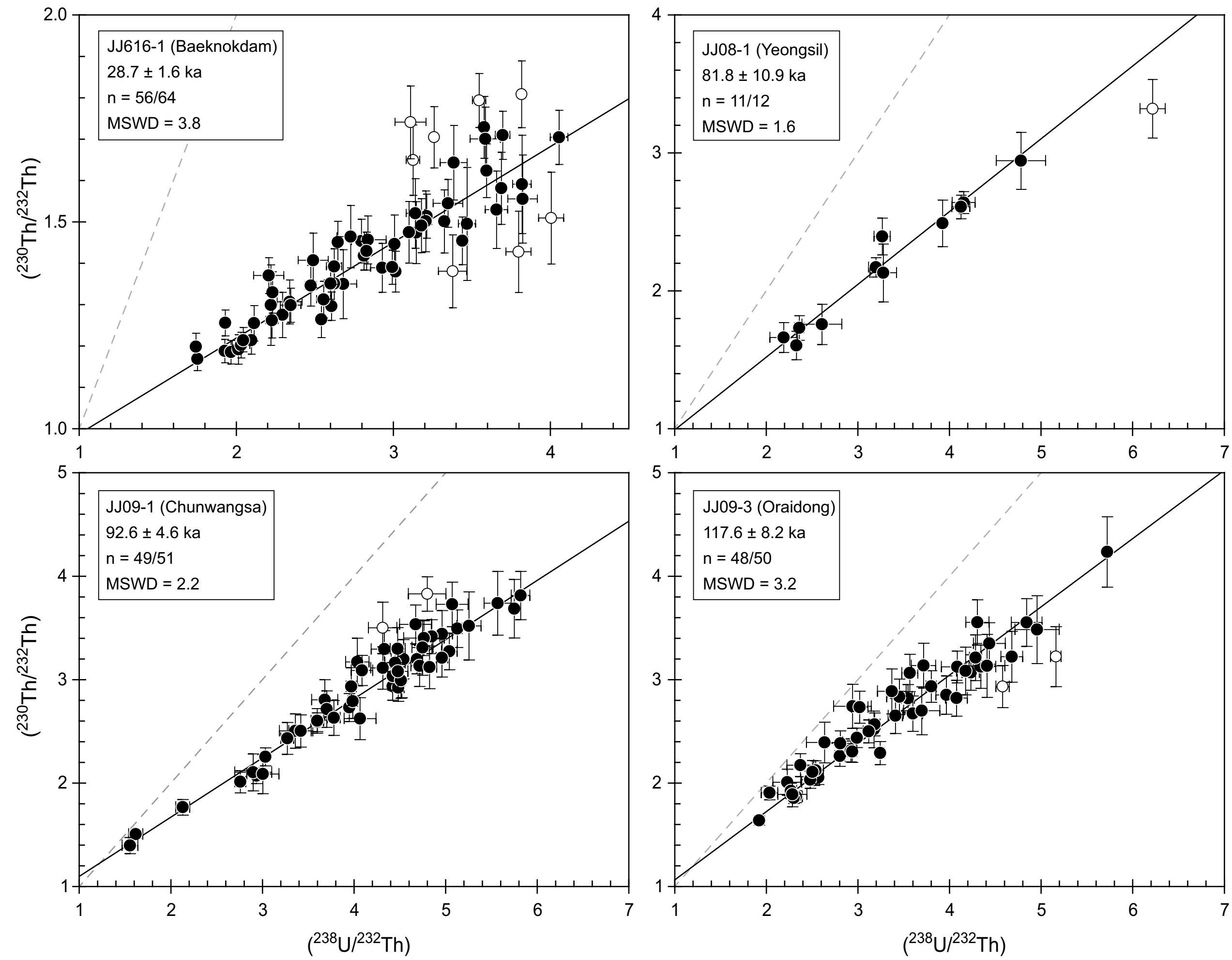

Fig. 3 Uranium–thorium isochron plots for Jeju zircons. The dashed gray lines depict the equiline. The open circles indicate outliers identified through the calculation of weighted mean age. Error bars represent 2 standard errors

weighted mean of 4,118 ± 22 ka (n = 22/25, MSWD = 5.7), confirming the significance of disequilibrium correction. The ^{232}Th-^{208}Pb dating may be less impacted by the disequilibrium effect. However, it should be noted that the measured ^{208}Pb/^{206}Pb ratios of the zircons and assumed common Pb ratio (= 2.0658; Stacey and Kramers 1975) indicate much higher fractions of common ^{208}Pb (f^{208}Pb$_c$) ranging from 39 to 79%. The ^{207}Pb-corrected ^{232}Th-^{208}Pb dates are scattered between 2.8 and 4.2 Ma, appearing much younger than the corrected ^{238}U-^{206}Pb age. This discrepancy principally resulted from high common Pb fraction, and the uncertainty in the common Pb isotopic composition. To achieve a more precise measurement of the Th-Pb age, it is essential to know the exact ^{208}Pb/^{206}Pb ratio of the common Pb in order to accurately determine the f^{208}Pb$_c$ (= [(^{208}Pb/^{206}Pb)$_{common}$/(^{208}Pb/^{206}Pb)$_{measured}$] × f ^{206}Pb$_c$).

As depicted in Fig. 4, the 61.308 zircon yields a disequilibrium- and common Pb-corrected weighted mean ^{238}U-^{206}Pb age of 2,488 ± 20 ka (n = 19/20, MSWD = 1.8) when assuming a magma Th/U ratio of 3.89 (the average Th/U of upper continental crust; Rudnick and Gao 2003). The ^{207}Pb-corrected common Pb fraction is determined to be 13–51% for ^{206}Pb and 42–95% for ^{208}Pb. It is worth noting that the 61.308 zircon initially consisted of three crystals (Wiedenbeck et al. 1995). The grains analyzed in this study may correspond to 61.308A, given their U (170 ± 85 μg/g) and Th (179 ± 151 μg/g) concentrations. The thermal ionization mass spectrometric ^{238}U-^{206}Pb and ^{232}Th-^{208}Pb ages of 61.308A zircon were reported as 2,488 ± 4 and 2,538 ± 10 ka, respectively (Wiedenbeck et al. 1995), which align with our measurements. Similar to the Penglai zircon, the ^{232}Th-^{208}Pb dates of 61.308 zircon exhibit significant scatter and appear to be younger than the ^{238}U-^{206}Pb age.

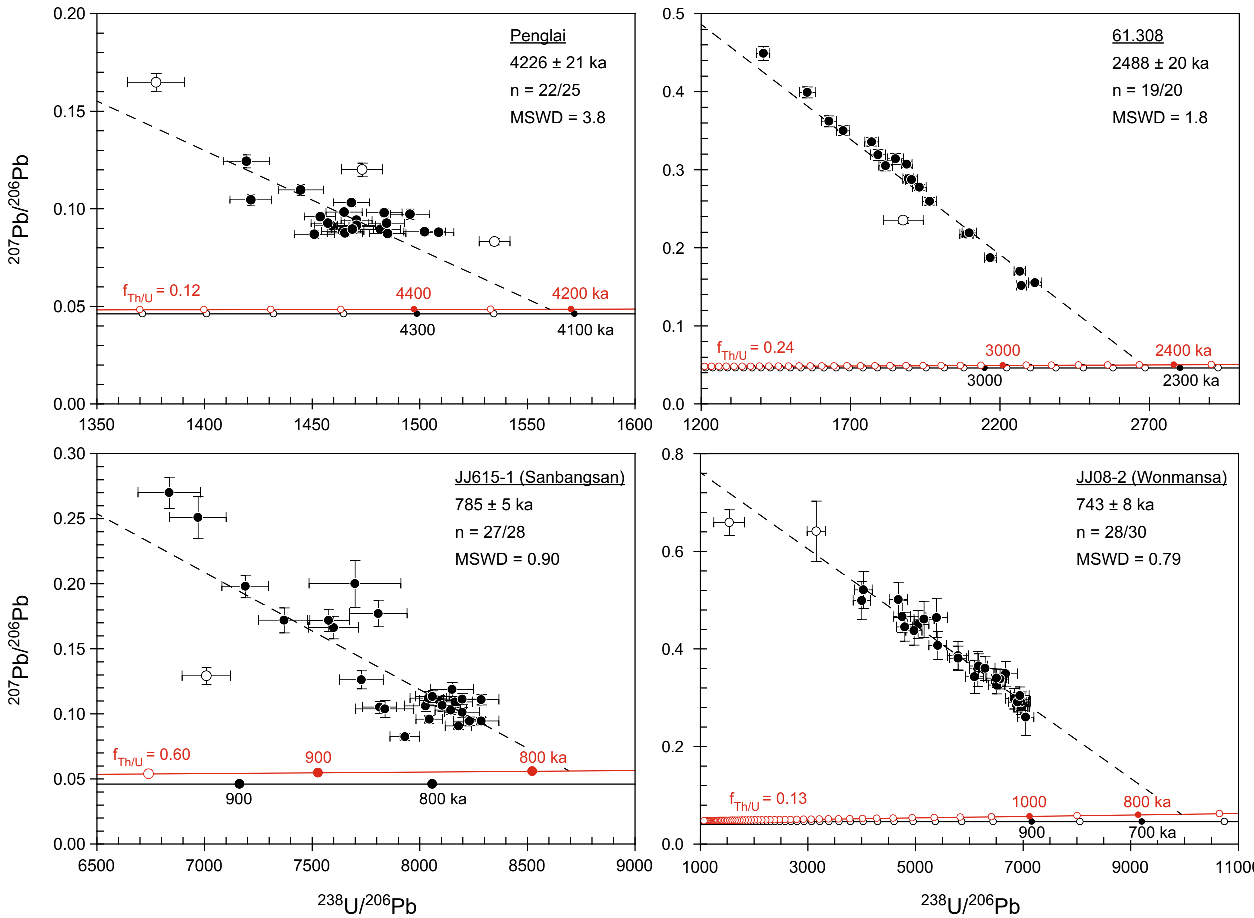

Fig. 4 Tera-Wasserburg plots for Jeju zircons and standards. Common Pb-uncorrected U-Pb data are plotted with the conventional (in black) and modified (in red) concordia curves. The open circle indicates an outlier identified through the calculation of weighted mean age. Error bars are at the 2σ level. Modified concordia curves are constructed following Sakata (2018), utilizing average $f_{Th/U}$ (= $(Th/U)_{zircon}/(Th/U)_{whole\text{-}rock}$) values. The numbers marked on the concordia curves represent dates in ka. Dashed lines on the plot depict the mixing lines between common and radiogenic Pb

The same correction scheme results in weighted mean common Pb and disequilibrium-corrected ^{238}U-^{206}Pb ages of 785 ± 5 ka (n = 27/28, MSWD = 0.90) and 743 ± 8 ka (n = 28/30, MSWD = 0.79) for the JJ615-1 and JJ08-2 zircons, respectively (Fig. 4). The $f_{Th/U}$ values were determined using the whole-rock Th/U ratios, and the $f_{Pa/U}$ and common Pb isotopic compositions were assumed to be consistent with those used for dating the Penglai and 61.308 zircon. The ^{207}Pb-corrected $f^{206}Pb_c$ is notably higher in the JJ08-2 zircons (0.44 ± 0.13) compared to the JJ615-1 zircons (0.11 ± 0.06). Despite the high common Pb fraction, the JJ08-2 zircons show a good fit of the mixing line between the radiogenic and common Pb (Fig. 4). On the other hand, the ^{207}Pb-corrected ^{232}Th-^{208}Pb dates of JJ615-1 zircons (727 ± 11 ka, n = 28, MSWD = 26) are younger and more scattered compared to the corrected ^{238}U-^{206}Pb dates. The Th-Pb dating method was not applicable for JJ08-2 zircon because ^{208}Pb in this zircon is predominantly composed of common Pb (average > 95%). The zircon U-Pb age of sample JJ615-1 marginally agrees with the whole-rock Ar-Ar age (802 ± 5 ka; Koh et al. 2013) of a trachyte collected from the Sanbangsan area. Interestingly, this age corresponds to the timing of the Matuyama/Brunhes magnetic reversal, defining the Early-to-Middle Pleistocene boundary (~780 ka). The zircon U-Pb age of sample JJ08-2 falls within the range of zircon dates (377–988 ka; Marsden et al. 2021) reported for a trachyte lava collected from the same locality.

Concluding remarks

This study employed femtosecond laser-connected MC-ICPMS to determine the U-Th and U-Th-Pb ages of Pleistocene zircons collected from Jeju Island, Korea. The obtained ages for these zircons and reference materials generally agree with the previously recommended ages. Our findings underscore the importance of applying radioactive disequilibrium correction when dating young (<5 Ma) zircons. Further investigations are required to enhance zircon Th–Pb dating by accurately measuring the common Pb isotopic composition.

Abbreviations

LA-MC-ICPMS	Laser ablation-multi-collector-inductively coupled plasma mass spectrometry
KBSI	Korea basic science institute
CL	Cathodoluminescence
MSWD	Mean squared weighted deviation

Supplementary Information

The online version contains supplementary material available at https://doi.org/10.1186/s40543-024-00427-3.

Additional file 1. Table S1 GPS coordinates and petrographic and mineralogic summaries of trachyte samples used for zircon extraction in this study.

Additional file 2. Table S2 Laser ablation MC-ICPMS instrument operational parameters for zircon U-Th and U-Th-Pb dating.

Additional file 3. Table S3 Whole-rock chemical composition of trachyte samples used for zircon extraction in this study

Additional file 4. Table S4 LA-MC-ICPMS U-Th concentrations and activity ratios of Jeju zircons.

Additional file 5. Table S5 LA-MC-ICPMS U-Th-Pb isotope data for Jeju zircons and standard zircons.

Additional file 6. Fig. S1 U-Th plot for zircon standards. The dashed line depicts the equiline shown for reference. Error bars represent 2 standard errors.

Acknowledgements

We thank Giun Han for his assistance in LA-MC-ICPMS measurements.

Author contributions

ACSC designed the research. USA, ACSC, and YJJ investigated the field outcrops and collected the samples. YJJ and MJJ conducted the experiments. ACSC and YJJ wrote the manuscript. All authors contributed to the interpretation of the results, and have read and approved the final manuscript.

Funding

This work was jointly supported by the National Research Foundation of Korea (NRF) grant funded by the Korean government (MSIT) (2021R1A2C1003363), and a KBSI grant (C380100), awarded to Albert Chang-sik Cheong.

Availability of data and materials

All data generated or analyzed during this study are included in this published article [and its supplementary information files].

Declarations

Competing interests

The authors declare that they have no competing interests.

Received: 11 September 2023 Accepted: 8 March 2024
Published online: 20 March 2024

References

Ahn US, Hong SS. Volcanological history of the Baengnokdam summit crater area, Mt. Halla in Jeju Island Korea. J Petrol Soc Korea. 2017. https://doi.org/10.7854/JPSK.2017.26.3.221.

Bacon CR, Persing HM, Wooden JL, Ireland TR. Late Pleistocene granodiorite beneath Crater Lake caldera, Oregon, dated by ion microprobe. Geology. 2000. https://doi.org/10.1130/0091-7613(2000)28%3c467:LPGBCL%3e2.0.CO;2.

Bernal JP, Solari LA, Gómez-Tuena A, Ortega-Obregón C, Mori L, Vega-González M, Espinosa-Arbeláez DG. In-situ ^{230}Th/U dating of quaternary zircons using LA-MCICPMS. Quat Geochronol. 2014. https://doi.org/10.1016/j.quageo.2014.06.003.

Black LP, Kamo SL, Allen CM, Davis DW, Aleinikoff JN, Valley JW, Mundil R, Campbell IH, Korsch RJ, Williams IS, Foudoulis C. Improved ^{206}Pb/^{238}U microprobe geochronology by the monitoring of a trace-element-related matrix effect: SHRIMP, ID-TIMS, ELA-ICP-MS and oxygen isotope documentation for a series of zircon standards. Chem Geol. 2004. https://doi.org/10.1016/j.chemgeo.2004.01.003.

Brenna M, Cronin SJ, Kereszturi G, Sohn YK, Smith IEM, Wijbrans J. Intraplate volcanism influenced by distal subduction tectonics at Jeju Island. Republic of Korea Bull Volcanol. 2015. https://doi.org/10.1007/s00445-014-0896-5.

Cheng H, Edwards RL, Shen CC, Polyak VJ, Asmerom Y, Woodhead J, Hellstrom J, Wang Y, Kong X, Spötl C, Wang X, Alexander EC Jr. Improvements in ^{230}Th dating, ^{230}Th and ^{234}U half-life values, and U–Th isotopic measurements by multi-collector inductively coupled plasma mass spectrometry. Earth Planet Sci Lett. 2013. https://doi.org/10.1016/j.epsl.2013.04.006.

Cheong ACS, Jeong YJ, Lee S, Yi K, Jo HJ, Lee HS, Park C, Kim NK, Li XH, Kamo SL. LKZ-1: a new zircon working standard for the in situ determination of U–Pb age, O–Hf isotopes, and trace element composition. Minerals. 2019. https://doi.org/10.3390/min9050325.

Diwakar PK, Harilal SS, LaHaye NL, Hassanein A, Kulkarni P. The influence of laser pulse duration and energy on ICP-MS signal intensity, elemental fractionation, and particle size distribution in NIR fs-LA-ICP-MS. J Anal at Spectrom. 2013. https://doi.org/10.1039/c3ja50088h.

Faure G, Mensing TM. Isotopes: principles and applications. 3rd ed. Hoboken: Wiley; 2005.

Feng R, Machado N, Ludden J. Lead geochronology of zircon by LaserProbe-Inductively coupled plasma mass spectrometry (LP-ICPMS). Geochim Cosmochim Acta. 1993. https://doi.org/10.2113/0530243.

Fryer BJ, Jackson SE, Longerich HP. The application of laser ablation microprobe-inductively coupled plasma mass spectrometry (LAM-ICP-MS) to in situ (U)–Pb geochronology. Chem Geol. 1993. https://doi.org/10.1016/0009-2541(93)90058-Q.

Gray AL. Solid sample introduction by laser ablation for inductively coupled plasma source mass spectrometry. Analyst. 1985. https://doi.org/10.1039/AN9851000551.

Guillong M, Günther D. Effect of particle size distribution on ICP-induced elemental fractionation in laser-ablation-inductively coupled plasma-mass spectrometry. J Anal at Spectrom. 2002. https://doi.org/10.1039/B202988J.

Guillong M, Schmitt AK, Bachmann O. Comment on "Zircon U–Th–Pb dating using LA-ICP-MS: simultaneous U–Pb and U–Th dating on 0.1 Ma Toya Tephra, Japan" by Hisatoshi Ito. J Volcanol Geotherm Res. 2015. https://doi.org/10.1016/j.jvolgeores.2015.03.003.

Guillong M, Sliwinski JT, Schmitt A, Forni F, Bachmann O. U–Th zircon dating by laser ablation single collector inductively coupled plasma-mass spectrometry (LA-ICP-MS). Geostand Geoanal Res. 2016. https://doi.org/10.1111/j.1751-908X.2016.00396.x.

Hirata T. Chemically assisted laser ablation ICP mass spectrometry. Anal Chem. 2003. https://doi.org/10.1021/ac020497q.

Hirata T, Nesbitt RW. U–Pb isotope geochronology of zircon: evaluation of the laser probe-inductively coupled plasma-mass spectrometry technique. Geochim Cosmochim Acta. 1995. https://doi.org/10.1016/0016-7037(95)00144-1.

Ho KS, Chen JC, Juang WS. Geochronology and geochemistry of late Cenozoic basalts from the Leiqiong area, southern China. J Asian Earth Sci. 2000. https://doi.org/10.1016/S1367-9120(99)00059-0.

Jackson SE, Günther D. The nature and sources of laser induced isotopic fractionation in laser ablation-multicollector inductively coupled plasma-mass spectrometry. J Anal at Spectrom. 2003. https://doi.org/10.1039/B209620J.

Jackson SE, Pearson NJ, Griffin WL, Belousova EA. The application of laser ablation-inductively coupled plasma-mass spectrometry to in situ U–Pb zircon geochronology. Chem Geol. 2004. https://doi.org/10.1016/j.chemgeo.2004.06.017.

Koh GW, Park JB, Kang BR, Kim GP, Moon DC. Volcanism in Jeju Island. J Geol Soc Korea 2013; UCI:G704-000209.2013.49.2.004.
Li XH, Long WG, Li QL, Liu Y, Zheng YF, Yang YH, Chamberlain KR, Wan DF, Guo CH, Wang XC, Tao H. Penglai zircon megacrysts: a potential new working reference microbeam determination of Hf–O isotopes and U–Pb age. Geostand Geoanal Res. 2010. https://doi.org/10.1111/j.1751-908X.2010.00036.x.
Lide DR, Frederikse HPR. CRC Handbook of Chemistry and Physics. 76th ed. Boca Raton, Florida: CRC; 1995.
Ludwig KR. Effect of initial radioactive-daughter disequilibrium on U–Pb isotope apparent ages of young minerals. J Res US Geol Surv. 1977;5:663–7.
Ludwig KR. User's Manual for Isoplot 3.75: A Geochronological Toolkit for Microsoft Excel. Berkeley Geochronology Center Special, Publication 5; 2012.
Le Maitre RW, Bateman P, Dudek A, Keller J, Lameyre Le Bas MJ, Sabine PA, Schmid R, Sorensen H, Streckeisen A, Woolley AR, Zanettin B. A classification of igneous rocks and glossary of terms. Oxford: Blackwell; 1989.
Marsden RC, Danišík M, Ahn US, Friedrichs B, Schmitt AK, Kirkland CL, McDonald BJ, Evans NJ. Zircon double-dating of Quaternary eruptions on Jeju Island, South Korea. J Volcanol Geotherm Res. 2021. https://doi.org/10.1016/j.jvolgeores.2020.107171.
Marsden RC, Danišík M, Schmitt AK, Rankenburg K, Guillong M, Ahn US, Kirkland CL, Evans NJ, Bachmann O, Tacchetto T, McDonald BJ, Olierook HKH. SS14-28: an age reference material for zircon U–Th disequilibrium dating. Geostand Geoanal Res. 2022. https://doi.org/10.1111/ggr.12406.
Mattinson JM. Anomalous isotopic composition of lead in young zircons. In: Carnegie Institution of Washington Year Book, vol. 72; 1973, p. 613–616.
Middlemost EAK. Naming materials in the magma/igneous system. Earth-Sci Rev. 1994. https://doi.org/10.1016/0012-8252(94)90029-9.
Paces JB, Miller JD Jr. Precise U–Pb ages of Duluth complex and related mafic intrusions, northeastern Minnesota: geochronological insights to physical, petrogenic, paleomagnetic, and tectonomagmatic processes associated with the 11 Ga midcontinent rift system. J Geophys Res. 1993. https://doi.org/10.1029/93JB01159.
Paton C, Hellstrom J, Paul B, Woodhead J, Hergt J. Iolite: freeware for the visualisation and processing of mass spectrometric data. J Anal at Spectrom. 2011. https://doi.org/10.1039/C1JA10172B.
Poitrasson F, d'Abzac FX. Femtosecond laser ablation inductively coupled plasma source mass spectrometry for elemental and isotopic analysis: are ultrafast lasers worthwhile? J Anal at Spectrom. 2017. https://doi.org/10.1039/C7JA00084G.
Poitrasson F, Mao X, Mao SS, Freydier R, Russo RE. Comparison of ultraviolet femtosecond and nanosecond laser ablation inductively coupled plasma mass spectrometry analysis in glass, monazite, and zircon. J Anal at Spectrom. 2003. https://doi.org/10.1021/ac034680a.
Reid MR, Coath CD, Harrison TM, McKeegan KD. Prolonged residence times for the youngest rhyolites associated with Long Valley Caldera: ^{230}Th-^{238}U ion microprobe dating of young zircons. Earth Planet Sci Lett. 1997. https://doi.org/10.1016/S0012-821X(97)00077-0.
Rudnick RL, Gao S. Composition of the continental crust. In: Rudnick RL, editor. The crust. Oxford: Elsevier; 2003. p. 1–64.
Russo RE, Mao X, Gonzalez JJ, Mao SS. Femtosecond laser ablation ICP-MS. J Anal at Spectrom. 2002. https://doi.org/10.1039/B202044K.
Sakata S. A practical method for calculating the U–Pb age of Quaternary zircon: correction for common Pb and initial disequilibria. Geochem J. 2018. https://doi.org/10.2343/geochemj.2.0508.
Sakata S, Hirakawa S, Iwano H, Danhara T, Guillong M, Hirata T. A new approach for constraining the magnitude of initial disequilibrium in Quaternary zircons by coupled uranium and thorium decay series dating. Quat Geochronol. 2017. https://doi.org/10.1016/j.quageo.2016.11.002.
Schärer U. The effect of initial ^{230}Th disequilibrium on young U-Pb ages: the Makalu case, Himalaya. Earth Planet Sci Lett. 1984. https://doi.org/10.1016/0012-821X(84)90114-6.
Sláma J, Košler J, Condon DJ, Crowley JL, Gerdes A, Hanchar JM, Horstwood MSA, Morris GA, Nasdala L, Norberg N, Schaltegger U, Schoene B, Tubrett MN, Whitehouse MJ. Plešovice zircon-a new natural reference material for U–Pb and Hf isotopic microanalysis. Chem Geol. 2008. https://doi.org/10.1016/j.chemgeo.2007.11.005.
Stacey JS, Kramers JD. Approximation of terrestrial lead isotope evolution by a two-stage model. Earth Planet Sci Lett. 1975. https://doi.org/10.1016/0012-821X(75)90088-6.
Steiger RH, Jäger E. Subcommission on geochronology: convention on the use of decay constants in geo- and cosmochronology. Earth Planet Sci Lett. 1977. https://doi.org/10.1016/0012-821X(77)90060-7.
Stirling CH, Lee DC, Christensen JN, Halliday AN. High-precision in situ ^{238}U-^{234}U-^{230}Th isotopic analysis using laser ablation multiple-collector ICPMS. Geochim Cosmochim Acta. 2000. https://doi.org/10.1016/S0016-7037(00)00457-9.
Sun SS, McDonough WF. Chemical and isotopic systematics of oceanic basalts. Geol Soc London Spec Publ. 1989. https://doi.org/10.1144/GSL.SP.1989.042.01.19.
Sylvester PJ, Jackson SE. A brief history of laser ablation inductively coupled plasma mass spectrometry (LA-ICP-MS). Elements. 2016. https://doi.org/10.2113/gselements.12.5.307.
Wiedenbeck M, Allé P, Corfu F, Griffin WL, Meier M, Oberli F, von Quadt A, Roddick JC, Spiegel W. Three natural zircon standards for U–Th–Pb, Lu–Hf, trace element and REE analyses. Geostand Newslett. 1995. https://doi.org/10.1111/j.1751-908X.1995.tb00147.x.
Wiedenbeck M, Hanchar JM, Peck WH, Sylvester P, Valley J, Whitehouse M, Kronz A, Morishita Y, Nasdala L, Fiebig J, Franchi I, Girard JP, Greenwood RC, Hinton R, Kita N, Mason PRD, Norman M, Ogasawara M, Piccoli PM, Rhede D, Satoh H, Schulz-Dobrick B, Skår Ø, Spicuzza MJ, Terada K, Tindle A, Togashi S, Vennemann T, Xie Q, Zheng YF. Further characterisation of the 91500 zircon crystal. Geostand Geoanal Res. 2004. https://doi.org/10.1111/j.1751-908X.2004.tb01041.x.
Woodhead JD, Horstwood MSA, Cottle JM. Advances in isotope ratio determination by LA-ICP-MS. Elements. 2016. https://doi.org/10.2113/gselements.12.5.317.
Yeo EY, Choi JH, Ahn US, Cheong ACS. Quartz OSL dating of palaeosols intercalated with basaltic lava flows and scoria deposits from monogenetic volcanoes in northeastern Jeju Island. Korea Geosci J. 2019. https://doi.org/10.1007/s12303-019-0010-2.
Yu S, Sun J, Evans NJ, Danišík M, Wu L, Tian Y, Shen Z. Further evaluation of Penglai zircon megacrysts as a reference material for (U–Th)/He dating. Geostand Geoanal Res. 2020. https://doi.org/10.1111/ggr.12331.

Publisher's Note